INSTITUTE OF PHYSICS PUBLISHING
Meas. Sci. Technol. 13 (2002) N31–N37

MEASUREMENT SCIENCE AND TECHNOLOGY
PII: S0957-0233(02)30394-1

DESIGN NOTE

Optical sensing of colour print on paper by a diffractive optical element

Jari Palviainen[1], Mika Sorjonen[2], Raimo Silvennoinen[1] and Kai-Erik Peiponen[1]

[1] Väisälä Laboratory, Department of Physics, University of Joensuu, FIN-80101 Joensuu, Finland
[2] Measurement and Sensor Laboratory, University of Oulu, Technology Park 127, FIN-87400 Kajaani, Finland

Received 1 November 2001, in final form 25 January 2002, accepted for publication 31 January 2002
Published 28 February 2002
Online at stacks.iop.org/MST/13/N31

Abstract
A diffractive optical element (DOE) based sensor was applied to investigate optical surface quality of two different commercial laser print papers before and after printing of red, green and blue colour ink. The DOE sensor provides simultaneously information on both reflected and transmitted light, whereas a spectrophotometer, which was applied as a corroborative method, yields non-simultaneous information about the total reflection and transmission from the samples. The DOE sensor images were analysed and information concerning the local anisotropy of the paper was obtained. The border between a colour print and non-print was also investigated using the DOE sensor and a microdensitometer. It is proposed that the DOE sensor provides better resolution of the border than the microdensitometer.

Keywords: reflectance, transmittance, diffractive optical element, paper print quality, paper surface, colour ink

1. Introduction

Traditionally paper is subject to mechanical testing which includes strength and roughness of paper. Various mechanical testing methods are defined in TAPPI standards. An interesting new technique for the assessment of the elastic properties of paper is based on laser ultrasonics [1]. There are various optical properties such as colour, opacity, brightness and gloss that are important in paper making and affect the final paper quality. The surface roughness of paper affects the reflectance and scattering of light from the paper surface and thus has a contribution for example to the quality of print on a paper [2]. For example, the gloss of paper strongly depends on the surface smoothness or roughness of the paper. In practice, parameters given by Kubelka–Munk theory [3, 4] specify the optical material and scattering properties of the paper. Light propagation in paper is typically a multiple-scattering phenomenon due to the complex nature of paper structure. Advanced light scattering models of paper require knowledge of the optical constants of the scattering particles such as fibres, fines and fillers, their aspect ratios and also particle package density. This complexity of parameters leads to the growing need for sophisticated tools capable of measuring accurate information on paper quality. Also, the anisotropy introduced by the papermaking process between the machine direction (MD) and cross-machine direction (CD) has its own influence on the optical spectra and on the spatial distribution of the scattered light intensity on the detection plane [5, 6].

As concerns the detection of print quality of paper various optical methods have been introduced for quality inspection. These include the traditional Chapman method [7], which involves determination of the contact area between paper and printing surface without ink, dynamic smoothness measurements of papers and print unevenness by laser beam reflection and microdensitometer [8] and confocal laser scanning microscopy [9]. Investigation of gloss and colour of paper prints has been also an important topic of research [10, 11].

0957-0233/02/040031+07$30.00

Our ideas on measurement of paper and print quality are based on the use of machine vision and intelligent optical sensors. In this paper we apply a diffractive optical element (DOE) sensor to the investigation of laser-light interaction with commercial paper before and after laser printing with colour ink. The DOE sensor has already been successfully used in the observation of optical surface quality of paper [12], print quality of black ink [13] and sensing of the surface quality of coated paper [14]. Also, it has been observed to be effective in other areas of material inspection [15, 16]. When ink has been printed onto a paper surface, the optical properties of the paper usually change on the area of the ink [17]. Using the image data provided by the DOE sensor, we detect the anisotropy of the surface roughness and also the specular reflection and transmission of the laser light from the print area. Here we measure also the spectral reflectance and transmittance of paper samples using a spectrophotometer (with an integrating sphere), and specify the three used laser print colours (red, green and blue). Finally we investigate the borders of the ink prints with the aim of determining the resolution of the DOE sensor when a microdensitometer is used as a corroborative method.

2. Theory of the DOE sensor

The imaging properties of the DOE sensor obey the laws of hologram imagery [18, 19]. The perfect reconstructing wavefront that diffracts from the present DOE forms a 4 × 4 light spot matrix in its focal plane as shown in figure 1. Using the theory of DOE sensors [20], we calculated the maximum radius of the deviation (SD) for a single spot in the image plane as shown in figure 2, when the diameter of the beam waist at the back surface of paper is evaluated at values of 0.2 and 1 mm. The optimization of the imaging properties can be performed following the procedure described in detail in our earlier work [21]. Thus, it is possible to avoid the overlapping of the intensity distributions of individual light spots in the DOE image.

The DOE, which was calculated by using the Rayleigh–Sommerfield diffraction integral [22], was an on-axis binary amplitude hologram and its transmission was adjusted to 50%. It consisted of a square array of 4 × 4 equispaced points as objects. The size of the DOE aperture was 4 mm × 4 mm and the focal length was 100 mm, while the distance between nearest adjacent spots in the focal plane was 125 μm, when the mean distance variable of reconstruction R_c was at infinity. High quality of the DOE was ensured by the use of an electron beam writer in the fabrication process of the present element.

3. Experiments and discussion

The paper sheets under investigation consisted of several sheets from two different types of commercial laser print paper with weight of 80 g m^{-2}. We measured the total reflectance (R) and transmittance (T) of all paper samples in the wavelength range 200–850 nm by using a Perkin Elmer λ18 spectrophotometer and SRS-99-020 white reflection standard. The diameter of the circular aperture of the spectrophotometer was 22 mm during the measurements. The uniform quality of each paper sample was verified by making measurements

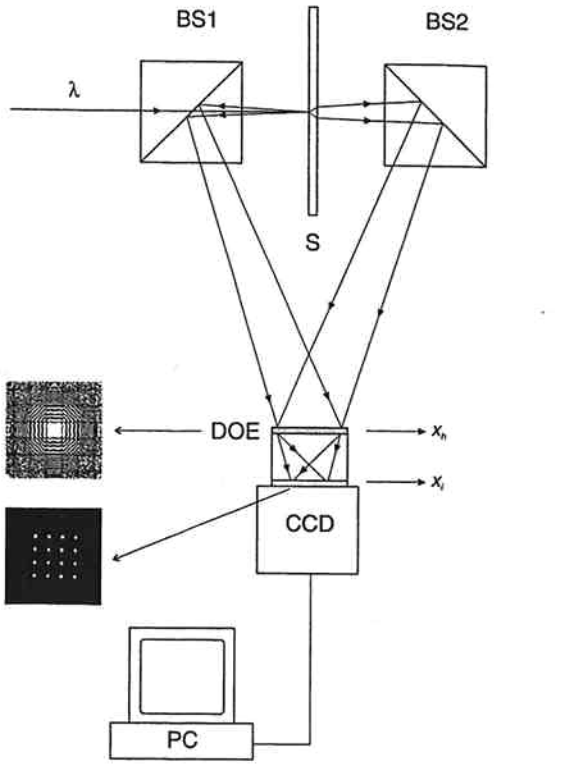

Figure 1. The setup of the DOE sensor. The wavefront (λ) from a laser propagates through the beam splitter (BS1) onto the surface of the paper sample (S). The reflected and transmitted light components are guided with beam splitters (BS1 and BS2) to the DOE aperture in the hologram plane (x_h–y_h plane), which diffracts the light components into the focal plane (x_i–y_i plane), where the CCD camera is located.

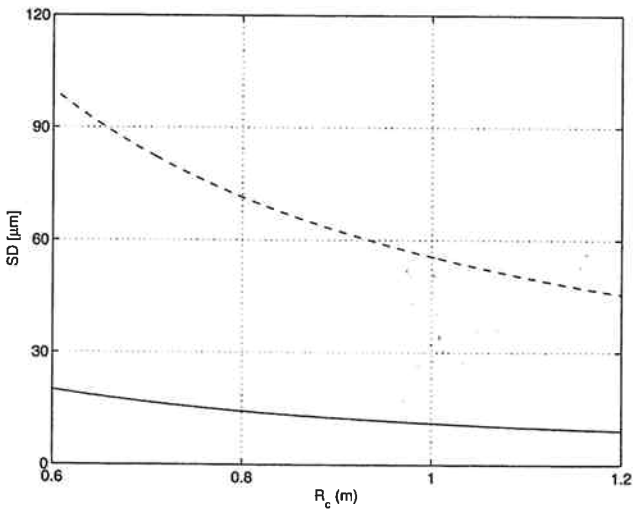

Figure 2. The maximum deviations of a single spot in the image plane as a function of mean distance R_c for diameters ($1/e^2$) of a scattering pattern of 0.2 mm (full curve) and 1 mm (broken curve) at the back surface of a 0.1 mm thick paper sample.

from several different locations before printing of ink. From figure 3 one may observe that the total responses for reflectance and transmittance measurements have a very high degree of uniformity for the same type of paper sheet. Even between two types of paper sheet the difference in spectral response is relatively small. The only considerable difference is in the UV region where the fluorescence from paper is generated [23].

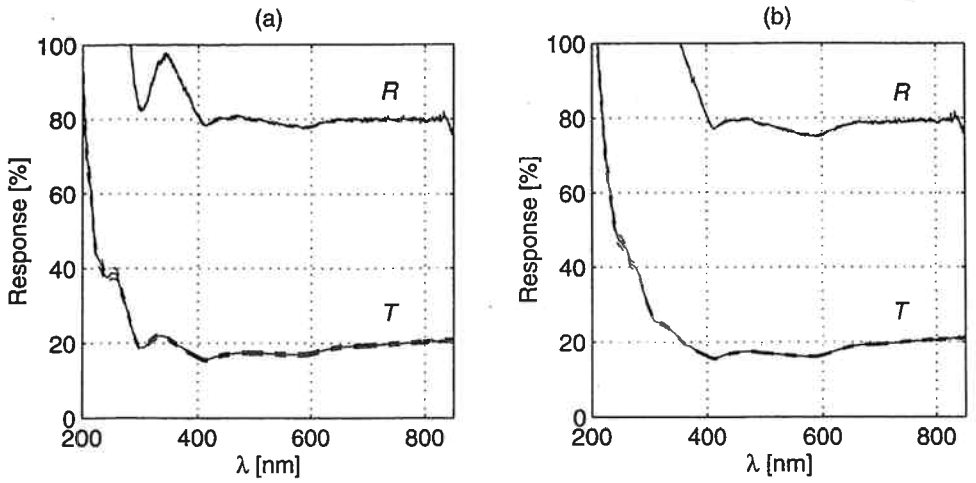

Figure 3. The mean reflectance R and transmittance T for paper samples of (a) type 1 and (b) type 2 (full curve). The standard deviation of reflectance and transmittance of the 36 spectra as a function of wavelength λ is represented around the mean responses (broken curve).

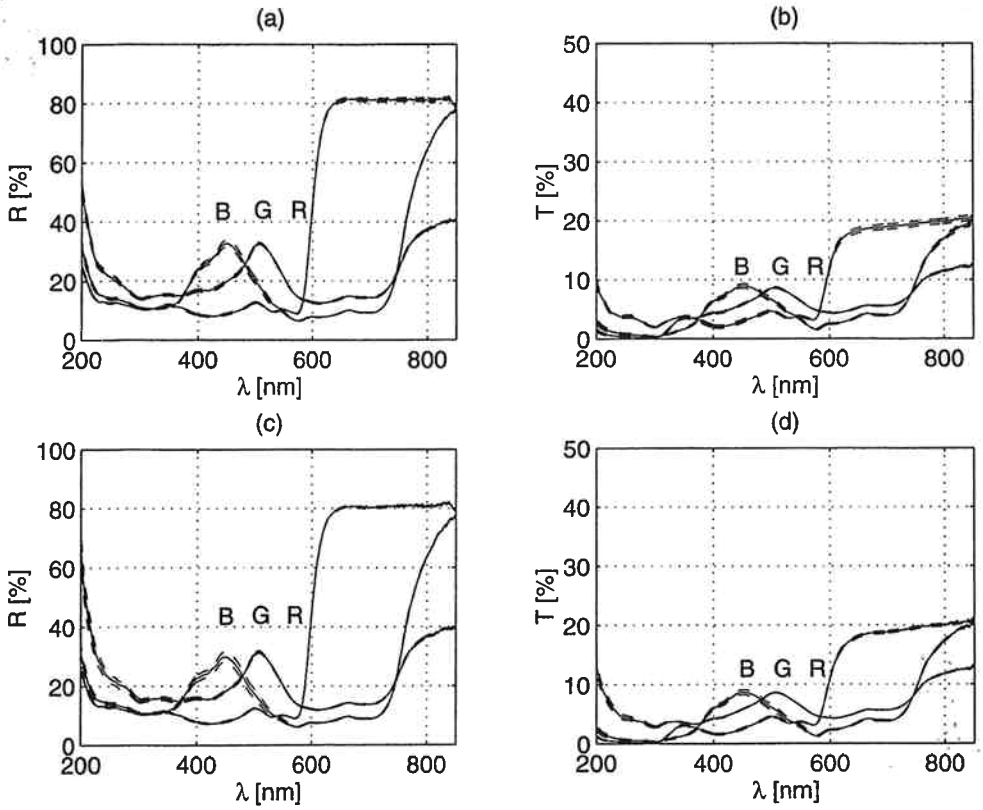

Figure 4. The mean (a) reflectance R and (b) transmittance T as a function of wavelength λ for paper samples printed with red, green and blue colours for type 1 paper (full curve). The responses for type 2 paper are shown in (c) and (d), respectively (full curve). The standard deviations of reflectance and transmittance of the 18 spectra are represented around the mean response value (broken curve).

The fluorescence is caused by optical brightness agents, which are used in some papermaking processes [24].

Next, we printed red, green and blue ink on each sample paper and specified the colours used in the RGB print with spectrophotometer measurements. The square area of print entirely covered the aperture of the spectrophotometer. In figure 4 the reflectance and transmittance spectra for both types of paper sample are shown. From figures 3 and 4 it is easily seen that the reflectance spectrum between white paper and paper printed with red ink are nearly the same in the wavelength range 630–850 nm. The same observation can also be made for the transmittance spectra. The fluorescence effect at wavelengths smaller than 400 nm is greatly diminished by printed ink.

Each sample was analysed by the DOE sensor shown in figure 1. We used a 17 mW linearly polarized HeNe-laser beam (λ = 632.8 nm), which was incident on the surface of the paper sample where the diameter of the beam waist was approximately 1 mm. Both reflected and transmitted wavefronts were simultaneously guided by beam splitters (BS1 and BS2) to the DOE aperture. The DOE itself was located 100 cm (= R_c) from the paper sample. The reflected and transmitted wavefronts were diffracted through the DOE aperture and focused onto different locations on its focal plane

where a CCD camera was located. In other words, images of the reflected and transmitted light are captured on the chip of the CCD, i.e. there is no objective lens. The scattering caused by the paper sample will change the wavefront from that of the perfect wavefront. The distortion of the wavefront results in the deformation of the image of the 4×4 spot matrix in the focal plane of the DOE. The deformed image patterns were analysed by a personal computer. With this kind of setup, where the DOE is used in off-axis reconstruction, the wavefronts are diffracted into separate locations of the focal plane without overlapping as we have shown in our earlier work [21].

We measured the paper samples before printing of colour ink from several locations with the aid of a linear translation stage controlled by a micrometer screw translation unit. The DOE sensor images were analysed by determining the mean intensity from a square area around each intensity peak in the 4×4 light spot matrix. The mean intensities of minima between the intensity peaks were calculated from areas of the same size. The size was defined so that there was no overlapping between minimum and maximum regions. We determined the visibility of the light spots in x_i and y_i directions of the image plane. The visibility values V_j were calculated from the formula

$$V_j = \frac{I_{\max} - I_{\min,j}}{I_{\max} + I_{\min,j}} \qquad (1)$$

where $I_{\max}$ is the mean of 16 intensity peak areas and $I_{\min,j}$ is the mean of the minimum areas between the intensity peaks in the j direction. Here j denotes the image plane direction x_i or y_i. From equation (1) it follows that the visibility value varies in the range from zero to unity. The orientation of paper samples was fixed so that the x_i direction coincided with the CD and the y_i direction coincided with the MD. We observed that the light spots in reflected and transmitted DOE sensor images are more broadened in the MD. This leads to the growth of the term $I_{\min,j}$ in equation (1), which lowers the visibility value in the MD. This difference between the MD and CD results from the fact that the angular distribution of light is larger in the direction of the paper machine. In papers there exists a preferential fibre orientation in the MD [5,6]. The DOE sensor is capable of sensing the difference between MD and CD, as observed by Sorjonen *et al* [13]. The results of the DOE sensor measurements before printing of ink are shown in table 1.

The next step was to examine the paper samples with the DOE sensor after printing of colour ink. The same DOE sensor setup was used as in figure 1 and measurements were made from exactly the same sample locations as earlier. The results are shown in table 2. First, we observe that there exists hardly any change in the DOE sensor images after printing of red ink. This is verified for both reflected and transmitted images. Neither the mean intensity values of peaks ($I_{\max}$) nor the visibility values in MD (V_{MD}) or CD (V_{CD}) exhibit any significant difference. This is caused by the negligible difference in reflectance and transmittance between white paper and paper printed with red ink at the used wavelength of 632.8 nm. This is in agreement with the spectrophotometer measurements shown in figures 3 and 4. Also, the $I_{\max}$ values for all print colours are in good agreement with spectrophotometer reflectance and transmittance measurements. This is also noticed from the correlation values $R_R^2 = 0.970$ and $R_T^2 = 0.973$ for type 1 paper, and for type 2 paper $R_R^2 = 0.976$ and $R_T^2 = 0.974$. However, the DOE sensor images from paper samples printed with green and blue ink showed different kinds of distribution in the image pattern. The visibility values have changed drastically from the case before printing of ink. It seems that the ink on the surface of the paper and the ink absorbed on the paper influence the reflected and transmitted wavefronts of light. As an example, in figure 5 are shown the reflected and transmitted DOE sensor images and their intensity plots in the MD and CD for a paper of type 1 printed with green ink. The visibility values for the light spot images in MD (V_{MD}) and CD (V_{CD}) in figure 5 were calculated to be 0.18 and 0.27 for the reflected image and 0.13 and 0.20 for the transmitted image, respectively. From figure 5 and the results of table 2 we clearly see that the differences between V_{MD} and V_{CD} values are distinctively smaller than they were before printing of green and blue ink. So, in this case the printed ink smoothes the difference of spatial distribution between the MD and CD.

Finally we focus our interest on the ink borders. For this purpose the borders were scanned with a Joyce Loebl 3CS double-beam microdensitometer. The width and height of the rectangular aperture was 50 and 150 μm, respectively, and the width of the aperture was set parallel to the scanning direction. As an example, in figures 6(a)–(c) are the microdensitometer scans made for type 1 paper sheet. Here it should be noted that the transmittances are not directly comparable to the spectrophotometer transmittances since the microdensitometer uses a white-light transmission.

Furthermore, the DOE sensor was used for the inspection of ink borders. The setup of the DOE sensor was the same as shown in figure 1, except the laser beam was focused by a lens ($f = 200$ mm) onto the surface of the paper. The diameter of the focused beam waist incident on the surface of the paper sample was calculated to be 160 μm at the $1/e^2$ level. With this setup DOE sensor images were grabbed at 100 μm intervals over the ink borders. The visibility values V_{MD} and V_{CD} were calculated from the image sets and the results are shown in figures 6(d)–(i). Due to the distance of the scan intervals and the width of the beam waist, the effect of the actual ink border on the light scattering can be distinguished on two grabbed images at maximum. Since the diameter of the beam waist was now considerably narrower, the spot deviation in the image plane is very small. Thus the overall visibility values are higher than before the use of a focusing lens.

In the case of red ink, we are not able to distinguish the ink border in either reflected or transmitted images. This was expected from the earlier spectrophotometer measurements. However, the green and blue ink borders are clearly seen as the visibility values diminish considerably. This means broadening of the intensity peaks in the 4×4 light spot image in both x_i and y_i directions. If we examine the difference in the visibility values between the MD and CD, we see that there is only a distinguishable difference in reflected images. Since the beam waist was focused to a much smaller area, the difference is not seen in transmitted images. This may be caused by the multiple scattering through the paper. In the case of reflected images from green and blue ink, we see clearly how the ink smoothes the difference in the spatial distribution

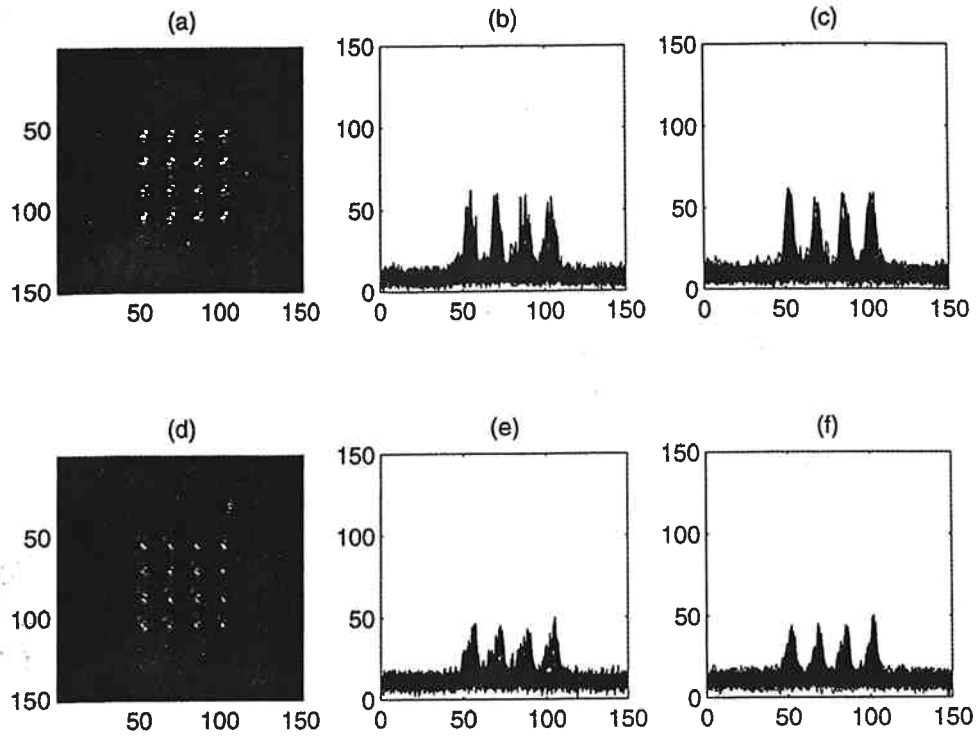

Figure 5. The 4 × 4 spot images obtained using the DOE sensor setup of figure 1 for a type 1 paper sample printed with green ink. Reflected (*a*) and transmitted (*d*) images and their corresponding intensity plots (*b*) and (*e*) parallel to the MD and (*c*) and (*f*) parallel to the CD. The numbers shown on the axes of the images and horizontal axes of plots are pixel numbers for distance, whereas numbers on the vertical axes of plots are for intensity on an eight-bit grey scale.

Table 1. Intensities and visibilities of the DOE sensor images for paper samples before printing of ink. Here the results are mean values for all samples. I_{max} is the mean value of the intensity peaks on an eight-bit grey scale, V_{MD} and V_{CD} are visibility values in the MD and CD, respectively. The subscripts 1 and 2 in reflected (R) and transmitted (T) modes denote the measurements made from two opposite sides of the paper. The standard deviations are denoted by the Δ-term.

	$R_1 \pm \Delta R_1$	$R_2 \pm \Delta R_2$	$T_1 \pm \Delta T_1$	$T_2 \pm \Delta T_2$
Paper #1				
I_{max}	78.77 ± 8.94	75.17 ± 7.00	49.53 ± 6.20	52.26 ± 6.16
V_{CD}	0.34 ± 0.04	0.33 ± 0.04	0.38 ± 0.05	0.38 ± 0.05
V_{MD}	0.19 ± 0.06	0.20 ± 0.06	0.22 ± 0.07	0.23 ± 0.06
Paper #2				
I_{max}	78.64 ± 8.60	82.48 ± 8.74	50.14 ± 7.16	50.73 ± 6.62
V_{CD}	0.34 ± 0.06	0.34 ± 0.04	0.38 ± 0.05	0.38 ± 0.05
V_{MD}	0.19 ± 0.06	0.22 ± 0.08	0.22 ± 0.08	0.21 ± 0.07

Table 2. Intensities and visibilities of the DOE sensor images for paper samples after laser printing of red, green and blue ink. Here the results are mean values for all samples. I_{max} is the mean value of intensity peaks on an eight-bit grey scale; V_{MD} and V_{CD} are visibility values in the MD and CD, respectively. The subscripts 1 and 2 in reflected (R) and transmitted (T) modes denote the measurements made for paper types 1 and 2, respectively. The standard deviations are denoted by the Δ-term.

		$R_1 \pm \Delta R_1$	$T_1 \pm \Delta T_1$	$R_2 \pm \Delta R_2$	$T_2 \pm \Delta T_2$
Red:	I_{max}	79.91 ± 8.94	47.31 ± 5.15	79.29 ± 8.07	44.72 ± 6.52
	V_{CD}	0.34 ± 0.04	0.37 ± 0.04	0.33 ± 0.05	0.34 ± 0.06
	V_{MD}	0.22 ± 0.06	0.21 ± 0.06	0.22 ± 0.05	0.23 ± 0.06
Green:	I_{max}	25.01 ± 3.03	19.58 ± 1.88	23.17 ± 2.46	18.85 ± 1.77
	V_{CD}	0.25 ± 0.05	0.20 ± 0.04	0.22 ± 0.05	0.20 ± 0.03
	V_{MD}	0.18 ± 0.05	0.13 ± 0.04	0.18 ± 0.05	0.10 ± 0.04
Blue:	I_{max}	7.40 ± 1.05	8.96 ± 1.26	6.98 ± 1.26	8.70 ± 0.99
	V_{CD}	0.26 ± 0.04	0.32 ± 0.07	0.25 ± 0.05	0.34 ± 0.05
	V_{MD}	0.19 ± 0.06	0.23 ± 0.06	0.20 ± 0.06	0.19 ± 0.06

of light scattering from the paper surface. The visibility values in the MD and CD are nearly the same. In figure 6, the data obtained from microdensitometer scans and from DOE sensor images are shown in their maximum variation range. We see that the DOE sensor is considerably more sensitive in distinguishing the ink border.

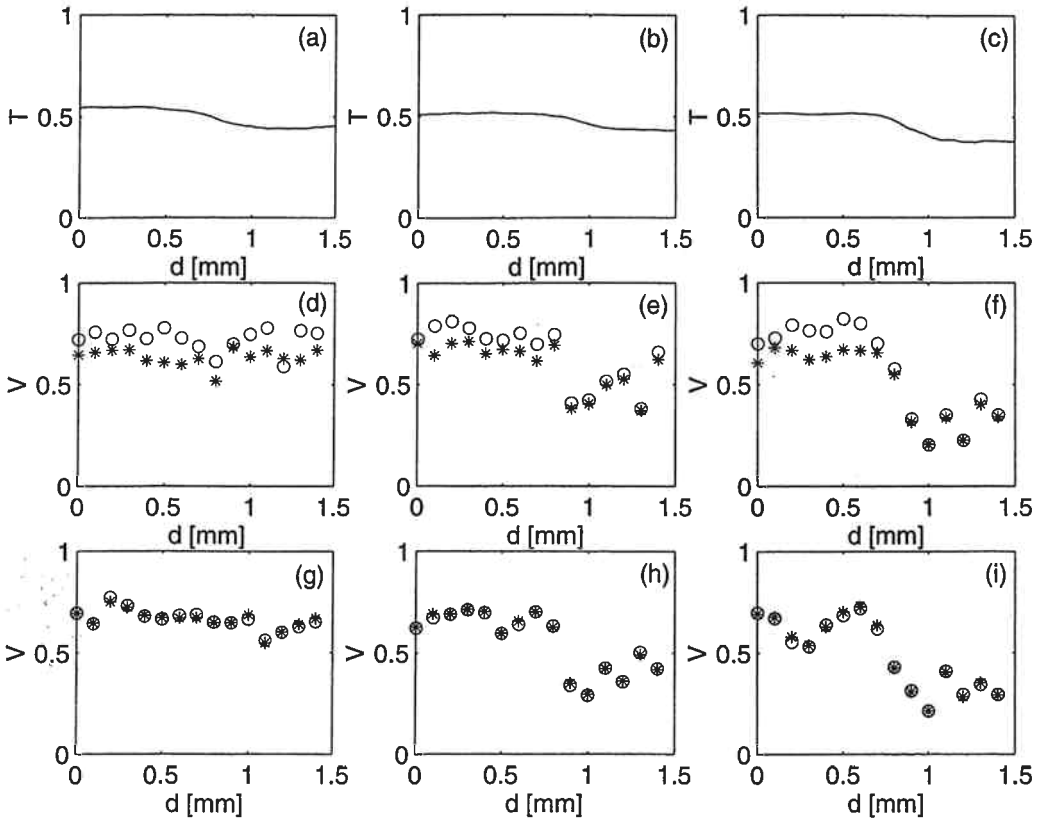

Figure 6. Microdensitometer scans for a type 1 paper sheet. The ink border of (*a*) red, (*b*) green and (*c*) blue colour as a function of measuring distance *d*. In (*d*)–(*f*) are shown the corresponding visibility values of reflected DOE sensor images. The visibility values for transmitted DOE sensor images are shown in (*g*)–(*i*). The visibility values in the MD and CD are denoted by a star and an open circle, respectively.

4. Conclusions

The DOE sensor was observed to be capable of sensing the anisotropy of the print paper between the MD and CD. The magnitude of anisotropy is possible to draw out from reflected or transmitted wavefronts of laser light that scatter from paper. It was also observed that the (R, G and B) colour print inks had influence on the reflectance, transmittance and optical anisotropy of the print paper. The intensity of the DOE sensor images showed correlation to spectral reflectance and transmittance of light from print paper as expected. The visibility of the DOE images revealed higher values in the CD. The visibility values of the images taken from the paper sample with print ink indicated lower values than those taken from the areas of paper without ink. Moreover, the difference in visibility values between the MD and CD was significantly smaller after printing of ink. This may indicate that the ink will match the refractive index of print paper, affecting uniform scattering of light from the structure of paper.

The aims of the use of the DOE sensor define most of the adjustable parameters such as used laser light wavelength, beam waist size and the distance of the element from a sample. The optimization of these parameters helps us to find the best solution for the inspection of a specific paper material property. As a final conclusion we state that the phenomena revealed and investigated by the present DOE sensor may help us to find novel tools for classification of print quality of paper.

Acknowledgments

JP thanks the Jenny and Antti Wihuri Foundation and JP and RS thank the Academy of Finland for financial support.

References

[1] Berthelot Y M and Johnson M A 1997 *Opt. Eng.* **36** 408–15
[2] Niskanen K (ed) 1998 *Paper Physics* (Jyväskylä: Fapet Oy)
[3] Kubelka P and Munk F 1931 *Z. Tech. Phys.* **12** 593–601
[4] Kubelka P 1948 *J. Opt. Soc. Am.* **38** 448–57
[5] Koukolas A A and Jordan B D 1994 *J. Pulp Pap. Sci.* **20** J55
[6] Koukolas A A and Jordan B D 1994 *J. Pulp Pap. Sci.* **20** J77
[7] Chapman S M 1954 *Pulp Pap. Mag. Can.* **55** 88
[8] Blokhuis G and Kalff P J 1976 *Tappi* **59** 107
[9] Mangin P J, Beland M-C and Cormier L M 1994 Paper surface compressibility and printing in 1994 *Int. Printing and Graphic Arts Conf.* pp 19–31
[10] Burlone D A 1984 *Color Res. Appl.* **9** 213–19
[11] Dalal E N and Natale-Hoffman K M 1999 *Color Res. Appl.* **24** 369–76
[12] Silvennoinen R, Peiponen K-E, Räsänen J, Sorjonen M, Keränen E J, Eiju T, Tenjimbayashi K and Matsuda K 1998 *Opt. Eng.* **37** 1482–7
[13] Sorjonen M, Jääskeläinen A, Peiponen K-E and Silvennoinen R 2000 *Meas. Sci. Technol.* **11** N85–8
[14] Silvennoinen R, Peiponen K-E, Sorjonen M, Tornberg J and Sumen J 2001 *Pap. Timber* **83** 395–9
[15] Silvennoinen R, Räsänen J, Savolainen M, Peiponen K-E, Uozumi J and Asakura T 1996 *Sensors Actuators* A **51** 117–23
[16] Peiponen K-E, Silvennoinen R, Räsänen J, Matsuda K and Tanninen V P 1997 *Meas. Sci. Technol.* **8** 815–8

[17] Leekley R M, Denzer C W and Tyler R F 1970 *Tappi* **53** 615
[18] Latta J N 1971 *Appl. Opt.* **10** 599–608
[19] Latta J N 1971 *Appl. Opt.* **10** 609–18
[20] Silvennoinen R, Peiponen K-E and Asakura T 1999 Diffractive optical elements in material inspection *The International Trends in Optics and Photonics ICO IV, Optical Metrology* part VI, ed T Asakura (Berlin: Springer) pp 282–93
[21] Palviainen J and Silvennoinen R 2001 *Meas. Sci. Technol.* **12** 345–52
[22] Nieto-Vesperinas M 1991 *Scattering and Diffraction in Physical Optics* (New York: Wiley)
[23] Bergström H and Carlsson J 1996 *Nordic Pulp Pap. Res. J.* **11** 48–55
[24] Neimo L (ed) 1999 *Papermaking Chemistry* (Jyväskylä: Fapet Oy)